Hindawi Publishing Corporation
International Journal of Spectroscopy
Volume 2010, Article ID 704183, 7 pages
doi:10.1155/2010/704183

Research Article

Measurement of the ^{87}Rb$[5P_{3/2}(F' = 3) - 5S_{1/2}(F = 2)]$ Effective Nonradiative Relaxation Rate near a Metallic Film

Jing Liu,[1,2] Yifan Shen,[1] and Kang Dai[1]

[1] *Department of Physics, Xinjiang University, Urumqi 830046, China*
[2] *School of Science, Xi'an Jiaotong University, Xi'an 710049, China*

Correspondence should be addressed to Yifan Shen, shenyifan01@sina.com

Received 30 March 2010; Revised 20 May 2010; Accepted 2 July 2010

Academic Editor: Wei Kong

We have studied the effective nonradiative relaxation rate of the hyperfine level ^{87}Rb$[5P_{3/2}(F' = 3)]$ near a metallic film with diode laser-induced retrofluorescence spectroscopy and saturated-absorption spectroscopy technique. The glass-vapor interface is considered as two distinct regions, a wavelength-thickness vapor layer joined to the surface and a more remote vapor region. The total experimental retrofluorescence signal $S^{ob}(\nu_L)$ is the summation of the signal originating from the far-field region $S^T(\nu_L)$ and the signal originating from the near-field region $s^n(\nu_L)$. Considering the thermalization of ^{87}Rb$(5P_{3/2})$ atoms in the far-field region, we can approximate $S^T(\nu_L)$ by using the vertical fluorescence signal near the entrance window. Thus we get the experimental hyperfine signal profile of ^{87}Rb in the near-field region. The value of the effective nonradiative transfer rate $A^{nf}_{F'=3\to F=2} = 2.3 \times 10^8 s^{-1}$ near the metallic film is relatively large compared to the spontaneous emission rate $A_{F'=3\to F=2} = 1.1 \times 10^7 s^{-1}$

1. Introduction

The experimental investigations of laser-induced retrofluorescence (backscattered fluorescence) spectroscopy at the interface between a glass cell surface and an optically thick Cs vapor have been reported [1–4]. The retrofluorescence spectroscopy method consists of measuring the light emitted at the boundary by excited atoms in the direction opposite to the exciting laser beam. In these researches, the authors have found that surface effects play a key role in atomic excitation energy transfer at the interface between the glass cell wall and the Cs vapor. The surface of glass cell window is covered by adsorbates and a slow penetration of Cs atoms, thus forming an electrically conductive thin layer on the glass surface, at a distance of a wavelength approximately, where the atomic photon emission interacts strongly with the surface, leading to the loss of the surface excitation energy by a nonradiative channel. Therefore, the excited atoms near the glass cell surface have a strong nonradiative decay. This fact makes the interface of glass-Cs-metal vapor a specific, nonnegligible structure in the study of atomic excitation nonradiative transfer.

In [3], the authors have studied the effective nonradiative relaxation rate of the hyperfine level Cs$[6P_{3/2}(F' = 5)]$ near a metallic film with diode laser retrofluorescence spectroscopy. In this work, we have measured the retrofluorescence signal associated with the 780.2 nm $(5P_{3/2} \to 5S_{1/2})$ resonant line at the interface between glass cell window and ^{87}Rb vapor at a temperature around 400 K. We have estimated the effective nonradiative decay rate of the $F' = 3 \to F = 2$ hyperfine spectral line of the retrofluorescence by analyzing the profile of the hyperfine level ^{87}Rb $[5P_{3/2}(F' = 3) \to 5S_{1/2}(F = 2)]$ near a metallic film based on the retrofluorescence sub-Doppler effect. The value of the effective nonradiative decay rate of the $F' = 3 \to F = 2$ hyperfine spectral line owing to the coupling of the excited ^{87}Rb atom with metallic surface of the glass cell window, which is compared with the values measured by Le Bris et al [1].

2. Experimental Setup

The diode laser-induced retrofluorescence spectroscopy method reported here is similar to the one described in [1]. Figure 1 shows a simplified picture of the experimental

setup, and a simplified energy-level diagram of ^{87}Rb is shown in Figure 2. A sealed cylindrical glass cell (5 cm long and 2.5 cm in diameter) contains a sample of ^{87}Rb (98.6%) and ^{87}Rb(1.4%). The cell (test cell) is embedded inside an oven whose temperature is kept at ~400 K. The temperature provides a sufficient Rb vapor pressure to measure the retrofluorescence spectra, but it is low enough to avoid introducing a large thermal noise background. A diode laser (Model DL100) from Toptica Photonics, with a bandwidth below 5 MHz, is used to excite the rubidium atoms from the $5S_{1/2}$ ground state to the $5P_{3/2}$ excited state around the 780.2 nm resonance line. The laser beam is roughly collimated and apertured such that its diameter at the cell is ~2.0 mm. Fine tuning of the laser frequency is achieved by variation of the laser current or temperature, and the resonance fluorescence signal is observed with a CCD camera. The laser beam is divided by two beam splitters. The reflected beams are used to fix the frequency of laser, and the transmitted beam is used to pump the ^{87}Rb vapor.

The calibration of laser frequency is determined with a reference Rb cell (^{87}Rb for 98.6%) in room-temperature by saturated-absorption spectroscopy technique [5]. Since the propagation of the laser beam through a reference cell is easily observed on the monitor at room temperature, the probe laser beam is allowed to pass through the rubidium reference cell onto a photomultiplier and recorded by a computer, and the power of probe laser beam is attenuated by a neutral density filter. Mirrors direct the counter propagating pump laser beam (~5 mW) through the reference cell. Counter propagating pump and probe beams overlap in a 5 cm long vapor cell with a crossing angle of about 15 mrad.

The transmitted beam (pump beam) derived from the diode laser is used to excite the ^{87}Rb atomic vapor around the 780.2 nm resonance line. Neutral density filter is used to attenuate the laser beam, and the laser power is weakened to 0.1 mW for a beam area of ~3 mm^2 for avoiding nonlinear effects. The laser beam is directed to the ^{87}Rb cell along the cell axis at an angle of ~2° with respect to the normal of the entrance window surface. The total fluorescence emitted backward, captured at an angle of ~13° with reference to the normal of the entrance cell window, is focused onto a 0.3 m focal-length optical multichannel analyzer (Model INS-300-122B). We define the vertical fluorescence which emitted at an angle of ~90° with respect to the normal of the entrance window surface near the entrance window (~5 mm) (see Figure 1). The vertical fluorescence is also measured simultaneously by the same OMA. Both two fluorescence signals are digitized and recorded by a computer.

Another experiment is carried out to confirm the thermalization of excited atoms in the vapor region far from the cell entrance window [5]. An counterpropagating diode laser (Model DL100) is used to probe the velocity distribution of excited atoms on the $5P_{3/2} \rightarrow 5D_{3/2}$ transition. Neutral density filter is used to attenuate the probe laser power to a few milliwatts. The probe laser beam is focused with a 0.6 m focal length lens to a Gaussian beam diameter of ~0.2 mm at the cell center. Over the length of the cell, the diameter of the probe laser beam does not vary significantly. For monitoring

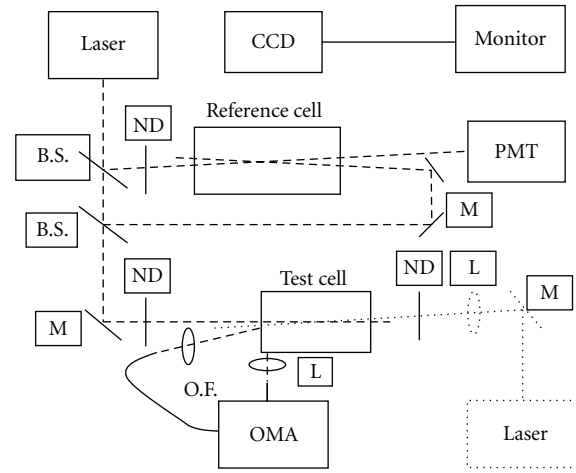

Figure 1: Schematic of the experimental setup. PMT, OMA, B. S., ND, O.F., M, and L represent photomultiplier, optical mutichannel analyzer, beam splitter, neutral density filter, optical fiber, mirror, and lens, respectively.

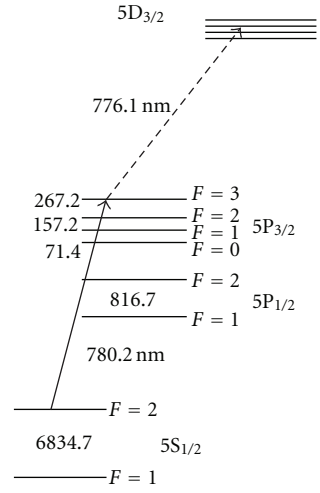

Figure 2: Schematic energy-level diagram of ^{87}Rb. Pump transition is indicated by a solid line and probe transition by a dashed line. Transition wavelengths are given in nm, and hyperfine splittings in MHz. Hyperfine level splittings have been greatly exaggerated to clarify and are not to scale.

the absorption of the probe laser, we detect fluorescence at the vertical direction to the probe laser propagating direction near the cell window. The fluorescence is focused on a 0.3 m focal-length OMA(Model INS-300-122B). When probing the $5P_{3/2} \rightarrow 5D_{3/2}$ transition, we have monitored $5D_{3/2} \rightarrow 5P_{1/2}$ fluorescence. Here, the pump laser is not attenuated by the neutral density filter.

3. Discussion

The authors of [1–4] have studied the integrated retrofluorescent spectral signals at the interface between a Cs vapor optically thick at resonance and a surface of glass

cell window. In the present case, we propose and carry out an experimental method allowing the measurement of the effective decay rate of the ^{87}Rb atomic $5P_{3/2}(F' = 3)$ hyperfine level in the presence of a near-metallic thin film. For this purpose, we have analyzed and discussed the spectral characteristic of the sub-Doppler cycling hyperfine $[5S_{1/2}(F = 2) \rightarrow 5P_{3/2}(F' = 3)]$ line, which is the strongest one of the structure in this section.

3.1. Geometric and Physical Description of the ^{87}Rb Vapor—Glass Window Interface. In this subsection, we briefly describe the geometrical and physical properties of the interface between the glass window and the optically thick saturated ^{87}Rb vapor irradiated with a laser, as described in [3]; see Figure 3.

According to experimental studies [6, 7], it appears that an alkali-metal atom can remain adsorbed on a standard glass window for a time largely exceeding the typical time of flight between the walls. Bouchiat and Brossel [6] had pointed out that the Rb vapor in a glass cell might not be in thermal equilibrium, especially near the glass surface, where rubidium atom might react with or be absorbed into the glass surface. Because of a slow penetration of Rb atoms and adsorbates inside of the glass and on its surface, we call the thin metallic Rb layer region (a). Between region (a) and the reservoir of Rb vapor, we consider a so-called near-field region (b) of dimension of the order of the wavelength (780.2 nm). In this wavelength-thickness layer, the atomic evanescent waves of the atomic $5^2P_{3/2}$ dipoles are strongly coupled with the metallic nanostructure surface [1]. Adjacent to the region (b), there are infinitely extended free ^{87}Rb atoms that we call the far-field region (c). In this region, excited atoms do not or hardly interact with the surface of glass cell. $S^T(\nu_L)$ designates the retrofluorescence signal from the far-field region (c), and $s^n(\nu_L)$ designates the integrated retrofluorescence sub-Doppler hyperfine signal originating from the near-field region. The total experiment retrofluorescence signal $S^{\text{ob}}(\nu_L)$ is the summation of $S^T(\nu_L)$ and $s^n(\nu_L)$.

3.2. Thermalization Processes in a Pure Rb Vapor. In this subsection, we have discussed the thermalization of the excited atom velocity distribution in a pure Rb vapor. Since the laser excited atoms with a Maxwell-Boltzmann velocity distribution, not all atoms are able to absorb the incoming radiation. Supposing that the laser beam propagates in z-direction, only those atoms (whose velocity component between v_z^- and v_z^+) can absorb the incoming photons.

$$v_z^{\pm} = \left[\nu_0^L - \nu_0 \pm \left(\Delta\nu_{\text{Lor}} + \frac{\Delta\nu_L}{2}\right)\right]\lambda_L, \tag{1}$$

where ν_0^L is the central frequency of laser, ν_0 is the central absorption frequency of the atom, $\Delta\nu_{\text{Lor}}$ is the full width of the Lorentzian line, $\Delta\nu_L$ is the linewidth of laser, and λ_L is the wavelength of laser.

In a pure Rb vapor, photon trapping processes and resonance exchange collisions [8] can lead to substantial thermalization of the excited atom velocity distribution.

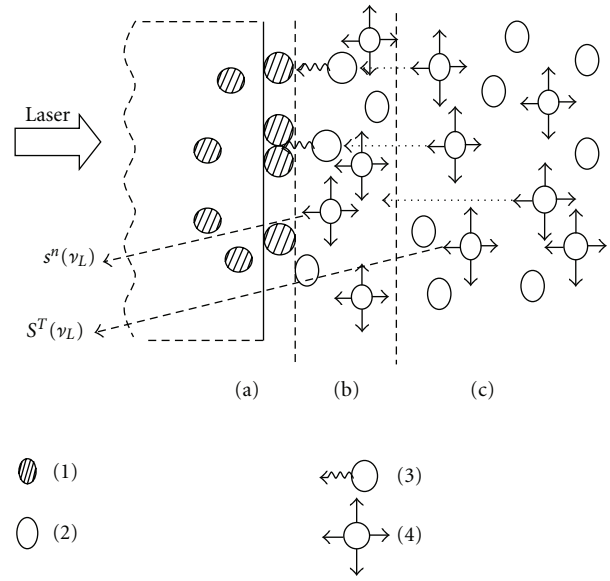

Figure 3: Physical and geometric description of the characteristic regions of the glass cell window and Rb vapor interface: (a) thin Rb metallic layer on the glass surface; (b) proximity region of the surface ($\sim \lambda$) called the near-field region of the interface; (c) the far-field region of the interface. $S^T(\nu_L)$ designates the integrated retrofluorescence signal from the far-field region of the interface. $s^n(\nu_L)$ designates the integrated retrofluorescence sub-Doppler hyperfine signal originating from the near-field region. The objects labeled (1)–(4) represent an atom adsorbed on the surface or on an Rb cluster, an Rb atom in the ground level, excited Rb atom undergoing a nonradiative relaxation, radiating (or fluorescent) atom, respectively.

The authors of [3] have noted that, in the vapor region far from the cell entrance window, the thermalization process by radiative trapping is more important than that of resonance exchange collisions.

In the case of a vapor layer confined in a thin layer ($\sim \lambda$) near the metallic film, one can expect that the thermalization due to radiation trapping will be reduced. We take the escape factor of the retrofluorescent photon $[5P_{3/2}(F' = 3) \rightarrow 5S_{1/2}(F = 2)]$ emitted from the near-field region close to 1; one can assume that a fraction of the population of a velocity class is not thermalized in the near-field region of the glass-Rb vapor interface. The spectral line has a Lorentzian-type profile [8]

$$s^n(\nu_L) \propto \frac{1}{[2(\nu_L - \nu_0)/\Gamma]^2 + 1}, \tag{2}$$

where Γ is the linewidth related to the total effective decay rate of the excited atoms in the near-field region.

Following to [8], we propose and carry out an experiment to explaine the thermalization of $\text{Rb}(5P_{3/2})$ atom in the far-field region. Figure 4. shows typical probe laser scans recorded on $5^2P_{3/2} \rightarrow 5^2D_{3/2}$ transition at different temperatures. From the chart, we can see obviously that $^{87}\text{Rb}(5P_{3/2})$ atom in the far-field region is thermalized at 400 K. At lower temperatures, the fluorescence maximum occurs when the pump laser is tuned near the peak of the

$5S_{1/2}(F=2) \rightarrow 5P_{3/2}(F'=3)$ transition, since this reduces the optical hyperfine pumping in the ground state.

3.3. Sub-Doppler Hyperfine Spectral Data Analysis and Discussion. In this subsection, we analyze the experimental hyperfine line profile of ^{87}Rb atom and obtain a Lorentzian-type profile of $^{87}\mathrm{Rb}[5P_{3/2}(F'=3) \rightarrow 5S_{1/2}(F=2)]$ transition in the near-field region.

Le Bris et al. [1] have given the total integrated retofluorescence with surface effects. We can get the retrofluorescence signal from the far-field region $S^T(\nu_L)$ with the following form [3], similarly.

$$S^T(\nu_L) \propto \alpha_T(\nu_L) \exp\left[-\overline{\tau}_T^f(\nu_L)\right] \times \int \frac{\alpha_T(\nu)}{\alpha_T(\nu_L)+\alpha_T(\nu)} \exp\left[-\overline{\tau}_T^f(\nu)\right] d\nu, \quad (3)$$

where $\alpha_T(\nu_L)$ is the normalized profile of the effective atomic absorption coefficient of the $F'=1,2,3$ hyperfine lines at the laser frequency ν_L; $\alpha_T(\nu)$ is the normalized profile of the effective atomic emission at frequency ν in the far-field region, where surface effects on the excited atoms are practically negligible; $\overline{\tau}_T^f(\nu_L)$ is the effective spectral optical thickness at laser frequency ν_L of the so-called stop-band filter [1] for the atomic hyperfine transition between the ground hyperfine level $F=2$ and the overall excited levels $F'=1,2,3$; and $\overline{\tau}_T^f(\nu)$ is the effective spectral optical thickness of the so-called stop-band filter at frequency ν.

We can obtain the integrated retrofluorescence sub-Doppler hyperfine signal $s^n(\nu_L)$, which originates from the near-field region, by subtracting the retrofluorescence signal $S^T(\nu_L)$ (given by (3)) from the total experiment signal $S^{\mathrm{ob}}(\nu_L)$. Because of the thermalization of $^{87}\mathrm{Rb}(5P_{3/2})$ atom in the far-field region at 400 K (see Figure 4), we can think approximately that the fluorescence radiance of excited atom in the far-field region is homogeneous. So we can approximate the far-field region signal $S^T(\nu_L)$ by using the vertical fluorescence signal which emitted at an angle of ~90° with respect to the normal of the entrance window surface near the entrance window (see Figure 1). We have

$$s^n_{\mathrm{exp}}(\nu_L) = S^{\mathrm{ob}}(\nu_L) - S^T(\nu_L). \quad (4)$$

Figure 5(a) shows the integrated resonance retrofluorescence signal $[S^{\mathrm{ob}}(\nu_L)]$ at the interface between glass window and ^{87}Rb vapor at a temperature ~127°C and laser power ~0.1 mW, when the diode laser is tuned over 780.2 nm ($5P_{3/2} \rightarrow 5S_{1/2}$) transition. Figure 5(b) shows the integrated vertical fluorescence signal $S^T(\nu_L)$ near the entrance window recording by the OMA simultaneously. Figure 5(c) shows a typical saturated absorption spectra for $^{87}\mathrm{Rb}[5S_{1/2}(F=2) \rightarrow 5P_{3/2}(F')]$ transitions at a room temperature. Four sub-Doppler features are seen, from the left they are $F=2 \rightarrow F'=2$, a crossover resonance ($F=2 \rightarrow F'=3,1$), a crossover resonance ($F=2 \rightarrow F'=3,2$), and the transition $F=2 \rightarrow F'=3$. We use them as reference frequency signal spectra. We have scaled the frequency axis by using the well-known gap between the two reference hyperfine lines $F'=3 \rightarrow F=2$ and $F'=2 \rightarrow F=2$ (value of 267 MHz), whose positions were determined by saturated absorption spectra. The frequency sweep is linear in the spectral band of interest.

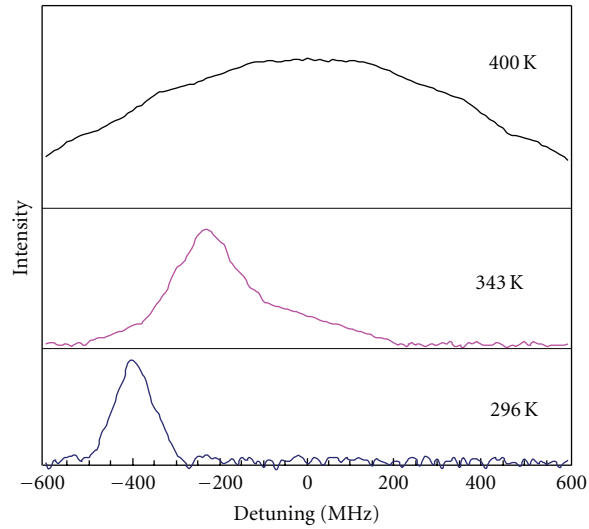

Figure 4: Excitation spectra probing the velocity distribution in the rubidium $5P_{3/2}$ state following pumping of the $5S_{1/2}(F=2) \rightarrow 5P_{3/2}(F'=1,2,3)$ resonance transition. The spectra are obtained by monitoring fluorescence on the $5D_{3/2} \rightarrow 5P_{1/2}$ transition, while scanning the probe laser over the $5P_{3/2} \rightarrow 5D_{3/2}$ transition. The position of the spike with respect to the pedestal depends on the detuning of the pump laser, which is set to maximize the total resonance fluorescence [8].

3.4. Results. We can get the hyperfine signal profile of ^{87}Rb in the near-field region by subtracting the value of $S^T(\nu_L)$ from the corresponding total experimental signal $S^{\mathrm{ob}}(\nu_L)$. The spectral distribution of points obtained by this method in the central area (~100 MHz spectral band centered on the line) and normalized to unity at the maximum is shown in Figure 6. The x axis is the laser frequency detuning from the hyperfine $F'=3 \rightarrow F=2$ line center. A fit of the normalized profile of data (Figure 6) corresponding to the spectral band (~100 MHz) centered on the cycling $F'=3 \rightarrow F=2$ hyperfine transition line is obtained by using a Lorentzian distribution function with a 48 MHz full width at half-maximum. The full width at half-maximum of the spectral profile obtained is estimated to be $\Gamma_{\mathrm{RF}} \sim 48$ MHz, and which is greater than the natural linewidth $\Gamma_n \sim 6.2$ MHz [9].

The experimental hyperfine sub-Doppler signal profile given in Figure 6 is reasonably fitted by relation (2), when Γ is identified with the experimental linewidth Γ_{RF} estimated to be 48 MHz. Thus Γ_{RF} is a spectral width, which is characteristic of the atomic excited level $5P_{3/2}(F'=3)$ in the near-field region. To characterize contributions of different relaxation processes contributing to the experimental retrofluorescent atomic line widthΓ_{RF}; in our elementary analysis we retain three dominant causes generating the relaxation of the excited level: the spontaneous emission process, the process of nonradiative transition of the atomic dipole due to the presence of the metallic film, and the

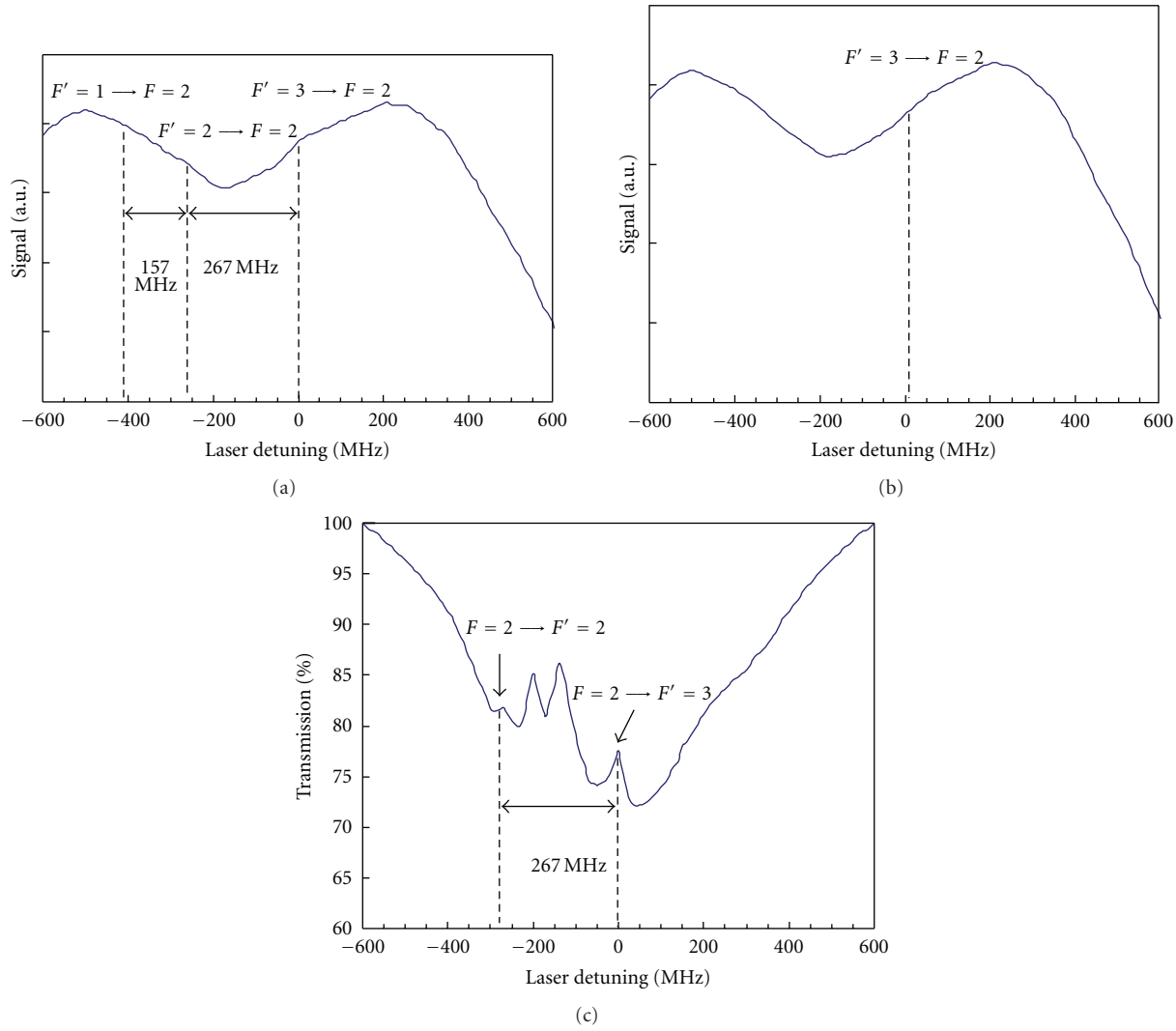

FIGURE 5: (a) Integrated 780.2 nm resonance retrofluorescence signal and (b) Integrated vertical fluorescence signal as a function of laser detuning from the resonance center for the $5S_{1/2}(F=2) \rightarrow 5P3/2(F'=1,2,3)$ transition obtained at a temperature ~400 K and laser power ~0.1 mW. (c) Experimental transmission spectrum for a room-temperature sample of ^{87}Rb atoms. The horizontal axis is the laser detuning in MHz relative to the $F=2 \rightarrow F'=3$ transition. Four sub-Doppler features are seen, from the left they are $F=2 \rightarrow F'=2$, a crossover resonance ($F=2 \rightarrow F'=3,1$), a crossover resonance ($F=2 \rightarrow F'=3,2$), and the transition $F=2 \rightarrow F'=3$.

resonant elastic collisions processes. Assuming that the relaxation probability is the same for all the excited atoms confined in the near-field region, and taking into account the competing relaxation processes of the $5P_{3/2}(F'=3)$ level, we sum up the corresponding spectral broadening and obtain the following relation [3]:

$$\Gamma_{\mathrm{RF}} = \Gamma_n + \Gamma_{\mathrm{coll}} + \Gamma_{nr}, \quad (5)$$

where Γ_{coll} is the resonance collisional broadening of the hyperfine line by the following expression [10]:

$$\Gamma_{\mathrm{coll}} = \frac{2\pi}{3} c_3 N, \quad (6)$$

where N is the number density of Rb atom in the ground state, and $c_3(8.5 \times 10^{-8}\,\mathrm{cm^3\,s^{-1}})$ is constant of interaction potential in the long-range region [10]. The Rb number density is determined by Gallaghers empirical formula [11]:

$$\log_{10}(N) = -\frac{A}{T} - (B+1)\log_{10} T + C + DT + 18.985, \quad (7)$$

where the Rb number density N is in $\mathrm{cm^{-3}}$. Values of the constants in (7) are $A=4302$, $B=1.5$, $C=11.722$, and $D=0$, respectively. Zhao et al. [12] have found that there is no systematic difference between the Rb number density near the surface ($\sim 10^{-5}$ cm) and that in the bulk. The Rb vapor number density near the cell window surface is $2.8 \times 10^{13}\,\mathrm{cm^{-3}}$ ($T=400$ K). Hence we obtain $\Gamma_{\mathrm{coll}} = 5.0$ MHz from (6).

Using the preceding experimental data, we deduce the spectral width associated with the nonradiative relaxation

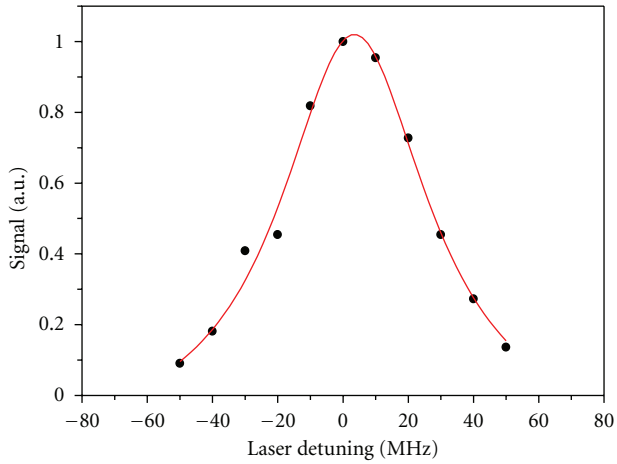

FIGURE 6: Distribution of the points around the $F' = 3 \rightarrow F = 2$ transition line center, obtained after subtracting $S^T(\nu_L)$ from the experimental retrofluorescence data. The solid curve is a Lorentzian fit of experimental points.

produced by the coupling of the excited atoms in the near-field region with the metallic film:

$$\Gamma_{nr} = \Gamma_{\mathrm{RF}} - \Gamma_n - \Gamma_{\mathrm{coll}} = 48 - 6.2 - 5.0 = 36.8\,\mathrm{MHz}. \quad (8)$$

We have $A^{nf}_{F'=3\rightarrow F=2} = 2\pi\Gamma_{nr} = 2.3 \times 10^8\,\mathrm{s}^{-1}$. The spontaneous emission rate of $5P_{3/2}(F' = 3) \rightarrow 5S_{1/2}(F = 2)$ is given by [13]

$$A_{F'=3\rightarrow F=2} = g_{F'=3,F=2} A_{5P_{3/2}(F')\rightarrow 5S_{1/2}(F=2)}, \quad (9)$$

where $g = 7/16$ is the statistical weight of the hyperfine $5P_{3/2}(F'=3)\rightarrow 5S_{1/2}(F = 2)$ transition and $A_{5P_{3/2}(F')\rightarrow 5S_{1/2}(F=2)} = 2.4 \times 10^7\,\mathrm{s}^{-1}$ [9, 13] is the spontaneous emission rate of $5P_{3/2}(F') \rightarrow 5S_{1/2}(F = 2)$. We have $A_{F'=3\rightarrow F=2} = 1.1 \times 10^7\,\mathrm{s}^{-1}$. The value of the effective nonradiative transfer rate $A^{nf}_{F'=3\rightarrow F=2} = 2.3 \times 10^8\,\mathrm{s}^{-1}$ is relatively large compared to the spontaneous emission rate $A_{F'=3\rightarrow F=2} = 1.1 \times 10^7\,\mathrm{s}^{-1}$. In [3], authors have reported the hyperfine level effective decay rate of $Cs[6^2P_{3/2}(F' = 5)]$ near a metallic film at a temperature of 403 K. They have the effective nonradiative transfer rate $A^{nf}_{F'=5\rightarrow F=4} = 3.0 \times 10^8\,\mathrm{s}^{-1}$ and the spontaneous emission rate $A_{F'=5\rightarrow F=4} = 1.14 \times 10^7\,\mathrm{s}^{-1}$. Compared to their work, we draw a consistent conclusion. The effective nonradiative transfer rate of excited atoms near the glass window is always larger than the relevant spontaneous emission rate. The morphology of the metallic film on the glass cell window is very complex, and we do not have the particular information about randomly distributed ^{87}Rb metallic clusters, atoms adsorbed on the clusters, and atoms chemically bonded to the surface. It is well known that the lifetime of an excited atom in the vicinity of a metallic film is influenced by its nature, thickness, complex dielectric constant, and other factors related to the surface effects modifying the nonradiative relaxation rate. Therefore, the satisfactory interpretation of the experimental results is an open problem of atomic spectroscopy all the same.

4. Conclusion

In conclusion, we have confirmed the existence of a sub-Doppler structure in the inhibition spectral band of the retrofluorescence signal, corresponding to the atomic $(5S_{1/2} \rightarrow 5P_{3/2})$ transition at the interface between glass window and saturated ^{87}Rb vapor at 400 K. Owing to a comparative analysis with the help of the saturated absorption spectroscopy method, we have indicated that the sub-Doppler hyperfine structure of this atomic transition coincides with the sub-Doppler structure observed in retrofluorescence. A particular analysis of the hyperfine $[5P_{3/2}(F' = 3) \rightarrow 5S_{1/2}(F = 2)]$ transition has been conducted to evaluate the influence of the presence of a metallic film at the interface for this atomic transition. In the near-field region, a fraction of the nonthermalized population of a velocity class plays an important role on the nature of the sub-Doppler profile. The population of a velocity class confined between the metallic film and the far-field region constitutes the effective population of radiating atoms originating from the sub-Doppler retrofluorescent signal. Using both the retrofluorescence and saturated absorption spectroscopy methods, we have measured the effect of the metallic film on the effective excited atom around the hyperfine level $5P_{3/2}(F' = 3)$ in the near-field region at 400 K. We have also indicated that the hyperfine spectral properties in the far-field region play the role of a photonic and atomic trap where the population of a velocity class and the resonant photons are thermalized.

Acknowledgment

This work was funded in part by the National Science Foundation of China under Grant no. 10964011.

References

[1] K. Le Bris, J.-M. Gagné, F. Babin, and M.-C. Gagné, "Characterization of the retrofluorescence inhibition at the interface between glass and optically thick Cs vapor," *Journal of the Optical Society of America B*, vol. 18, no. 11, pp. 1701–1710, 2001.

[2] J.-M. Gagné, K. Le Bris, and M.-C. Gagné, "Laser energy-pooling processes in an optically thick Cs vapor near a dissipative surface," *Journal of the Optical Society of America B*, vol. 19, no. 12, pp. 2852–2862, 2002.

[3] J.-M. Gagné, C. K. Assi, and K. Le Bris, "Measurement of the atomic $Cs[6^2P_{3/2}(F_e = 5)]$ hyperfine level effective decay rate near a metallic film with diode laser retrofluorescence spectroscopy," *Journal of the Optical Society of America B*, vol. 22, no. 10, pp. 2242–2249, 2005.

[4] K. Le Bris, C. K. Assi, and J.-M. Gagné, "Spectroscopic investigation of sensitized-Cs $(6^2P_{3/2} - 6^2P_{1/2})$ laser retrofluorescence in a pure optically thick vapour near a dissipative surface," *Canadian Journal of Physics*, vol. 82, no. 5, pp. 387–402, 2004.

[5] D. A. Smith and I. G. Hughes, "The role of hyperfine pumping in multilevel systems exhibiting saturated absorption," *American Journal of Physics*, vol. 72, no. 5, pp. 631–637, 2004.

[6] M. A. Bouchiat and J. Brossel, "Relaxation of optically pumped Rb atoms on paraffin-coated walls," *Physical Review A*, vol. 147, pp. 41–54, 1965.

[7] S. Briaudeau, D. Bloch, and M. Ducloy, "Sub-Doppler spectroscopy in a thin film of resonant vapor," *Physical Review A*, vol. 59, no. 5, pp. 3723–3735, 1999.

[8] J. Huennekens, R. K. Namiotka, J. Sagle, Z. J. Jabbour, and M. Allegrini, "Thermalization of velocity-selected excited-state populations by resonance exchange collisions and radiation trapping," *Physical Review A*, vol. 51, no. 6, pp. 4472–4482, 1995.

[9] C. E. Theodosiou, "Lifetimes of alkali-metalatom Rydberg states," *Physical Review A*, vol. 30, no. 6, pp. 2881–2909, 1984.

[10] K. Niemax and G. Pichler, "New aspects in the self-broadening of alkali resonance lines," *Journal of Physics B: Atomic and Molecular Physics*, vol. 8, no. 2, pp. 179–184, 1975.

[11] A. Gallagher and E. L. Lewis, "Determination of the vapor pressure of rubidium by optical absorption," *Journal of the Optical Society of America*, vol. 63, no. 7, pp. 864–869, 1973.

[12] K. Zhao, Z. Wu, and H. M. Lai, "Optical determination of alkali metal vapor number density in the vicinity (10^{-5}cm) of cell surfaces," *Journal of the Optical Society of America B*, vol. 18, no. 12, pp. 1904–1910, 2001.

[13] C. Vadla, V. Horvatic, and K. Niemax, "Radiative transport and collisional transfer of excitation energy in Cs vapors mixed with Ar or He," *Spectrochimica Acta B*, vol. 58, no. 7, pp. 1235–1277, 2003.